



Assessing the effects of solid wire electrode extension (stick out) increase in MIG/MAG welding

Régis Henrique Gonçalves e Silva¹ · Luiz Eduardo dos Santos Paes¹ · Rafael Costa Barbosa¹ · Francisco Sartori¹ · Mateus Barancelli Schwedersky¹

Received: 10 June 2017 / Accepted: 5 December 2017 / Published online: 15 January 2018
© The Brazilian Society of Mechanical Sciences and Engineering 2018

Abstract

In conventional MIG/MAG welding process, the root of some of the most frequent problems is related to current variation due to solid wire electrode extension (stick out) alteration. This becomes most relevant in semi-automatic welding procedures, where the welding operator is responsible for holding the torch. Inevitably, the contact tip-to-workpiece distance, and as a result, the stick out length, will oscillate due to operational difficulties, such as complex geometry and out-of-position welding. Since the average current has decisive influence over various weld properties, variations in its values incur in reduction of process and weld regularity, repeatability, robustness and reliability. The present work investigates and quantifies the effects such as current drop and electrode temperature profile based on well-known theoretical-analytical concepts under an application oriented standpoint, so as to scientifically support research and development of modern MIG/MAG welding adaptive systems. Results pointed a higher wire preheating degree in spite of lower current levels when stick out is increased. Experiments showed a weld bead geometrical reduction, which can be avoided through an intelligent system, capable of identifying welding current behavior, electrode voltage fall and electrical resistance curves for process online correction and prevention of possible defects.

Keywords GMAW · Semi-automatic welding · Current drop · Mathematical modelling · Adaptive system

1 Introduction

Industry demand on high productivity welding processes has encouraged the development of mechanized, and even automated systems. However, a significant portion of industrial applications in this sector still relies on operators (welders) for manual procedure execution, either for weld complexity or for lack of mechanization technology, with its inherent drawbacks. Besides all problems associated with occupational health and productivity, final product quality is often affected.

Semi-automated conventional MIG/MAG welding can be cited as an example. Variations in the Contact Tip-to-

Workpiece Distance (CTWD) are common when complex geometries are present, as well as in out of position welding and cause process instabilities. Sometimes, it is acceptable. In some joint tracking sensors, this is not only acceptable, but also necessary, since the control system relies on comparisons of transient current values triggered by torch movement [1]. However, in applications involving higher degree of sensitiveness (changing gap, thin sheet, root pass, etc.) and responsibility, inspection is critical, and defects due to those changings must be avoided.

Torch movement reflects in CTWD and stick out variation. The last one corresponds to the distance between the electric contact tube and electrode extremity. Stick out modification leads to changes on the welding circuit electrical resistance. To solve this problem, some manufacturers have recently added adaptive systems to their equipment, able to monitor and correct immediately such fluctuations and restore the stable condition automatically.

Robßmann [2] presents a system that uses wire feed speed and high dynamic motors to execute the required correction. Cruz et al. [3] applied sophisticated control and

Technical Editor: Márcio Bacci da Silva.

✉ Luiz Eduardo dos Santos Paes
luiz.paes@posgrad.ufsc.br

¹ Department of Mechanical Engineering, Welding Laboratory, Federal University of Santa Catarina, Florianópolis, Santa Catarina, Brazil

acquisition image techniques with hybrid Neuro-Fuzzy artificial intelligence systems, to adjust process parameters in real time. Nele et al. [4] compared the results obtained with Neuro-Fuzzy algorithms with linear regression models for automatic welding parameters correction, and concluded that the first had a better performance.

Adaptive systems are also present in pulsed MIG/MAG welding. Saraev [5] showed that in these cases, correction can be made through pulse duration. Mvola et al. [6] evaluated an equipment that operates with combined transfer (short-circuit and free flight), which correction principle is based on a pre-defined short-circuit percentage in a pulse sequence. Yan et al. [7] implemented a Fuzzy controller that reacts to disturbances and keeps penetration in the desired level using average current control. All systems above required a previous numerical and experimental study to identify most efficient parameters for correction.

In this context, the present work aims at a new approach of the main effects of stick out variation in conventional MIG/MAG process considering free flight metal transfer mode (spray), and as a result supports scientific–technological research and development of modern adaptive systems. Specifically, the paper presents a theoretical–analytical scope for observation and quantification of the stick out change impacts (due to CTWD oscillation) on welding, as a basis to develop MIG/MAG process control methods when operated in circumstances that lead to welding torch height variations. For this, thermal and electrical behavior modeling, (taking into account the correspondent and pertinent simplifications) and comparisons between simulation and experimental results were set as objectives.

1.1 Effects due to solid wire electrode extension (stick out) increase

There are many consequences of stick out increase. However, some of these are more relevant for welding practical aspects than others. The main effects are described below.

1.1.1 Thermal changes

In welding power source with constant voltage static characteristic, adjusted variables are welding voltage (U_{ref}) and wire feed speed (V_a). Therefore, current intensity is a consequence of both [8]. When the distance between torch and piece increases, and as a result the stick out, circuit electrical resistance grows up. This affects electrical conduction and modifies current intensity, as shown in Fig. 1 [9].

The empirical equation proposed by Lesnewich (Eq. 1) [10] suggests that electrode melting in the MIG/MAG

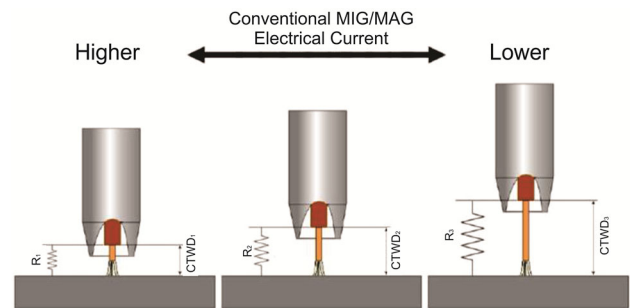


Fig. 1 Electrical current as a function of different CTWD in conventional MIG/MAG process [9]

process with reverse polarity has two predominant components: the anodic heating, due to kinetic energy and electron condensation energy, and the resistive heating due to current flow, known as Joule effect.

$$V_a = \alpha I_m + \beta L(I_{ef})^2 \quad (1)$$

In Eq. (1), V_a corresponds to wire feed speed, I_m to average current, I_{ef} to effective (RMS) current and L to stick out length. If metal transfer occurs in free flight (spray) mode, average current becomes numerically equal to effective current and can be named welding current. The constants α and β are associated to material composition and diameter, and represent the portions related to anodic heating and Joule heating, respectively.

Analyzing the mathematical expression above for the same wire speed, which can be equal to wire fusion rate, as stick out length grows up, the portion distribution associated with anodic heating and Joule heating changes. Considering a voltage–power source static characteristic, in spite of current drop showed in Fig. 1, the greater the stick out, greater is the correspondent Joule effect portion, with a reduction in the fraction due to anodic heating. An investigation headed by French [11] proved that stick out increase in self-shielded flux cored arc welding (FCAW) generates higher intensity Joule preheating and can lead to an electrode temperature variation from 300 to 1000 °C.

The preheating level for each stick out length can be determined theoretically solving the energy balance equation proposed by Waszink and Van Den Heuvel [12] (Eq. 2). In this case, heat transfer is determined by Joule effect and thermal conduction. The solution displays electrode temperature profile after specifying boundary conditions, material properties and process parameters.

$$\frac{d}{dz} \left(k(T) \frac{dT}{dz} \right) + V_a \rho \frac{d}{dz} (cp(T)T) = -j^2 r(T) \quad (2)$$

In Eq. (2), V_a corresponds to electrode wire speed, ρ to specific mass, j to current density, $k(T)$ to thermal conductivity, $cp(T)$ to specific heat and $r(T)$ to electrical resistivity. As shown, physical properties are temperature

dependent. Then, in spite of the advantage of being ease to solve mathematically when using constant k , cp and r coefficients, the result would not be appropriate for real-world requirements.

Figure 2 presents a schematic including specified boundary conditions. In electrode tip ($z = 0$), material lies in fusion temperature, T_f . On the other extreme ($z = L$), which accounts for electrical contact tube, temperature is T_c .

The model above assumes the following simplifications:

- (a) Temperature does not vary in the direction perpendicular to wire axis.
- (b) Wire moves with a constant feed speed.
- (c) Temperature distribution is due to a stationary regime. In other words, temperature is not time dependent.
- (d) Transition solid–liquid point remains the same and is located at $z = 0$.

1.1.2 Voltage drop and electrode electrical resistance

A higher stick out length promotes welding circuit impedance increase, as shown in Fig. 1. Experimentally, this is recognized through current drop. It is also possible to calculate ohmic resistance, as well as voltage drop. Temperature profile is needed, which can be obtained from described methodology in item 1.1.1., since electrical resistivity is not constant. Equations (3) and (4) regards to voltage drop $|\Delta V(z)|$ and electrical resistance R , respectively [13].

$$|\Delta V(z)| = \int_0^L \left(\frac{r(z)I}{S} \right) dz \tag{3}$$

$$R = \frac{\Delta V}{I} \tag{4}$$

Electrical resistivity is temperature dependent and has a value for each electrode (z) point. Therefore, it can be

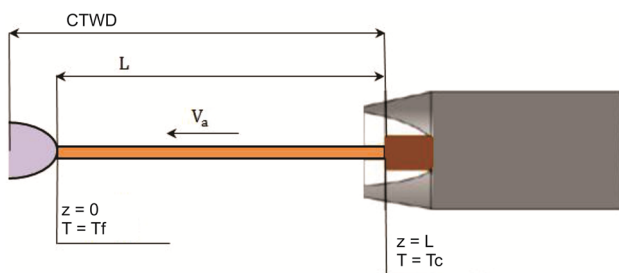


Fig. 2 Boundary conditions for energy balance equation. Adapted from [9]

expressed as a function $r(z)$. Variable S regards to electrode cross section, and variable I , to welding current.

1.1.3 Bead geometry

Stick out increase has a direct influence on welding bead geometry, since current intensity is reduced. Lower current means lower magnetic field and lower pressure over welding pool. The mechanism associated with droplet impact on base metal with determined mass and velocity (momentum) is also affected. Droplet speed is dependent on welding current [14]. Essers and Walter [15] found in experiments that droplet mass increases when current goes down. However, both transfer frequency and speed achieve lower values. Consequently, they also contribute to reduce penetration level. Kim and Na [16] results attest the described evidence through different CTWD trials. Weld pool temperature profile and correspondent surface tension profile are also affected by current, with impact in wettability and bead geometry [17].

2 Materials and methods

To investigate the effects due to stick out increase, prescribed methodology was divided into two different approaches. The first one, which can be classified as a theoretical, was based on mathematical analysis of Lesnewich equation (Eq. 1), and energy balance equation (Eq. 2). The obtained results were then related to the second approach, which has an experimental track.

To compute current drop, Eq. (1) was used with α e β coefficients from literature [18] for carbon steel (AWS ER70S6) considering a 1.2 mm diameter wire. The study was focused in a free flight transfer (spray) mode. Then, average current I_m becomes numerically equal to effective current I_{ef} , and can be named welding current I . Equation (5) is resultant from Eq. (1) manipulation.

$$\alpha I + \beta L(I)^2 - V_a = 0 \tag{5}$$

The second-order equation was solved for the same wire speed of $V_a = 7.7$ m/min, varying stick out length L in the range from 1 to 40 mm. The positive root represents balance current, which corresponds to associated current after ohmic resistance increase due to an increase in L value.

After finding each balance current, stick out values of 5, 10, 15 and 20 mm were selected for a detailed study, since this domain corresponds to most usual one in practical terms of MIG/MAG welding. Equation (2) was used to compute wire temperature profile, which is related directly to Joule effect contribution, and thereby to preheating degree. It is important to emphasize that physical properties such as thermal conductivity k , specific heat cp and

electrical resistance r are temperature dependent. Their respective curves were taken from literature data of low carbon steel [19].

To show properties relevance, Eq. (2) was solved using constant coefficients (values for room temperature) as well as using variable coefficients through Finite Element Method implementation. Boundary conditions of Fig. 2 were specified as: steel melting temperature, $T_f = 1538$ °C [19] and electric contact tube temperature $T_c = 77$ °C [13].

With electrode temperature profile for each of the four selected stick out, voltage drop (Eq. 3) and electrical resistance (Eq. 4) were calculated using trapezoidal numerical integration.

Experimental stage consisted of bead on plate welding for CTWD of 7, 12, 17 and 20 mm, with wire speed V_a of 7.7 m/min and reference voltage U_{ref} of 26 V. When CTWD is varied, stick out length also changes, as verified in preliminary high speed camera tests and is located in the most usual range (5–20 mm) [20]. Therefore, current drop and bead geometry can be related. The experimental stage consisted of bead on plate welding for CTWD of 7, 12, 17 and 20 mm, with V_a feed speed of 7.7 m/min and reference voltage U_{ref} of 26 V. Current drop and bead geometry can be related. Welding power source “IMC MTE Digitec 800”, with 16 kVa power, and current capacity of 800 A was selected. All tests were performed with a water-cooled MIG/MAG commercial torch with current capacity of 450 A, perpendicular to work piece surface. A steel electrode (AWS ER70S6) of 1.2 mm diameter was used. Shielding gas selected was Ar-2% O₂, with 17 l/min flow rate. Steel plates had dimensions 250 × 100 × 6.5 mm. Welding torch movement was done with a six-axis robot with 900 mm/min in all cases. Current and voltage signals were measured with a “IMC SAP 4.0” acquisition system, just above the electrode, in the torch. This is the optimum point for acquisition, the nearest place of arc able to collect data. After welding, cross section of each sample was analyzed through a macrography procedure using Nital 5% etching.

3 Results and discussion

The first assessed effect regards to current drop. From Eq. (5), decreasing behavior was possible to predict when stick out length incremented. For 1–40 mm range, current drop had a nonlinear profile, as shown in Fig. 3.

Figure 3 domain, which correspond to 1–40 mm range, is not inherent to practical welding application. Usually, stick out values vary from 5 to 20 mm. A detailed analysis was conducted with values from Table 1, resultant from Eq. 5.

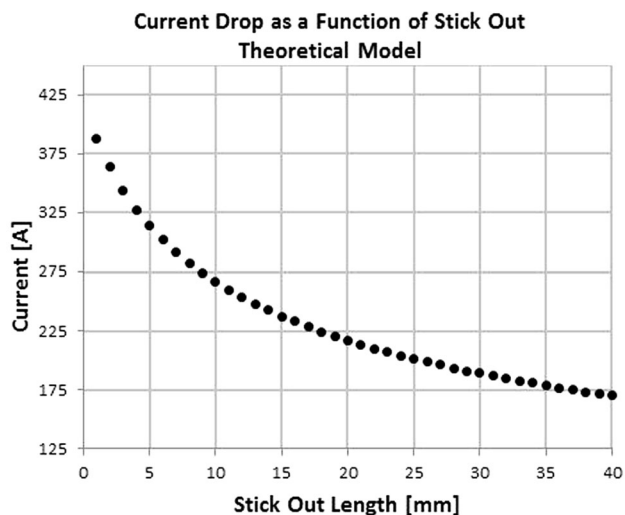


Fig. 3 Theoretical current drop curve as a function of stick out length

Table 1 Theoretical welding current values correspondent to studied stick out lengths

Stick out (mm)	Current (A)
5	314
10	267
15	238
20	217

Due to a higher electrode preheating when stick out length is incremented, temperature distribution changes. Equation (2) solution for specified boundary conditions results in the following profile. However, physical properties are temperature dependent and not constant coefficients. Figure 4a shows temperature profile considering constant thermal conductivity k , specific heat cp and electrical resistivity r , while Fig. 4b shows temperature profile considering the correspondent variable coefficients.

As predicted, greater preheating degree due to Joule effect contribution for high stick out values led to a temperature increase for both constant and variable coefficients. Two regions can be identified in the graphics above: the larger one starts at the electrode contact tube and is mainly influenced by Joule effect heating. The second, located at the electrode extreme, corresponds to anodic heating and promotes a sharp temperature pattern due to arc heat. Another fact is that, for the same stick out, absolute value was greater when variable coefficients were used. Besides that, Fig. 4b curve presented a less linear profile, if compared to Fig. 4a. Voltage drop and electrode electrical resistance were quantified through Eqs. (3) and (4), considering temperature dependent resistivity and, therefore, variable through stick out length. Figure 5a presents the result obtained for voltage drop, and Fig. 5b, for electrical resistance. The relation between voltage drop and stick out, as well as between electrical resistance and

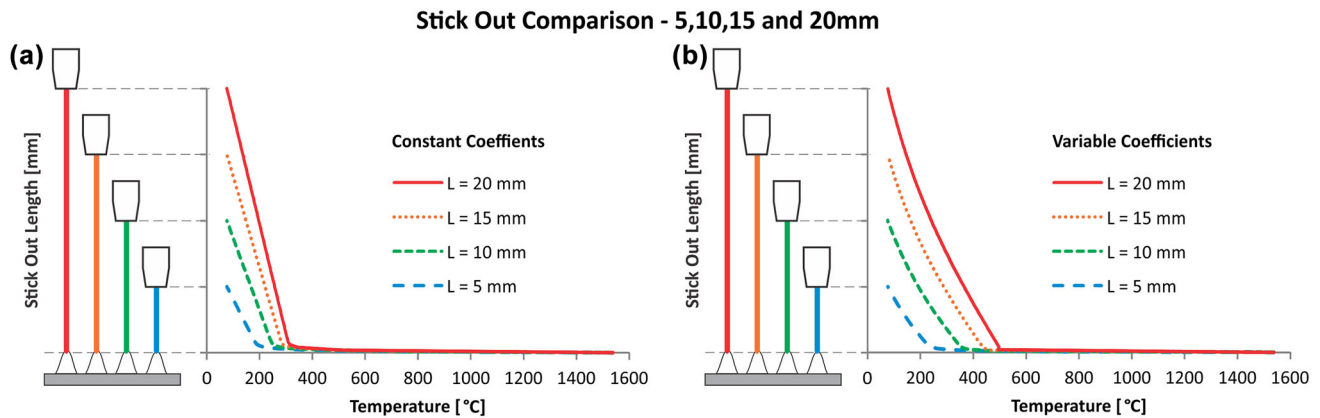


Fig. 4 Electrode temperature profile for stick out length of 5, 10, 15 and 20 mm. **a** Constant coefficients. **b** Variable coefficients

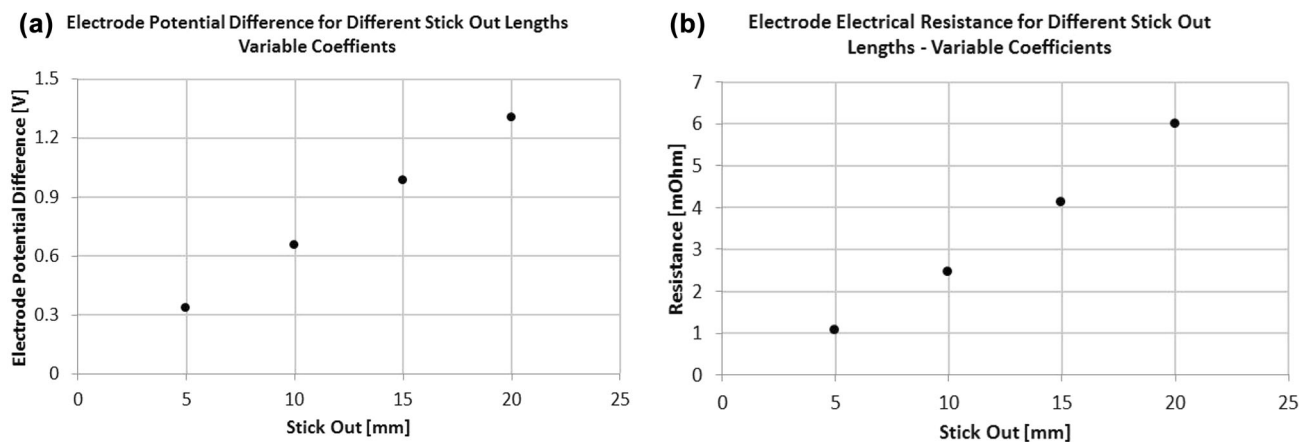


Fig. 5 **a** Electrode potential difference as a function of stick out. **b** Electrode electrical resistance as a function of stick out. Stick out values of 5, 10, 15 and 20 mm

stick out, for the specified range, has a linear pattern, although electrical resistivity depends on temperature based on a third-degree polynomial equation.

Experimental stage focused on the relation between current drop curve and weld bead geometry for different CTWDs, and consequently, different stick out lengths. Four CTWDs were chosen based on usual welding values. In Fig. 6, current drop can be approximated of a straight line. Current intensity varied from 343 ± 22.8 A, with 7 mm, to 252 ± 1.4 A, with 20 mm CTWD. This represents a 7.0 ± 1.4 A/mm reduction. In theoretical data of Fig. 3, current oscillated from 314 A, with 5 mm stick out, to 217 A, with 20 mm. Therefore, current drop was 6.5 A/mm. Through statistical hypothesis tests, it is not possible to affirm that those current rates are different.

Resultant welding bead were assessed for each CTWD. Average values of three samples for electrical current, penetration, width, total fusion zone area and dilution are present in Table 2.

Due to current drop as CTWD increases, weld bead penetration varied from 2.74 mm with CTWD = 7 mm, to 1.92 mm with CTWD = 20 mm. Dilution oscillated from 56%, with CTWD = 7 mm, to 41% with CTWD = 20 mm. This fact can be explained based on lower magnetic forces, magnetic field and lower arc pressure over the weld pool. Besides that, due to lower current intensity, correspondent momentum was also reduced and softened droplet impact over base metal. Even though, finger shape format was present thanks to Argon shielding gas. Macrographies for each CTWD are displayed in Fig. 7.

4 Conclusions

CTWD and correspondent stick out variations in welding procedure, which is usual in manual, but also possible in mechanized applications, have significant impact on weld bead geometry and means to minimize resulting

Fig. 6 Experimental current drop curve as a function of CTWD

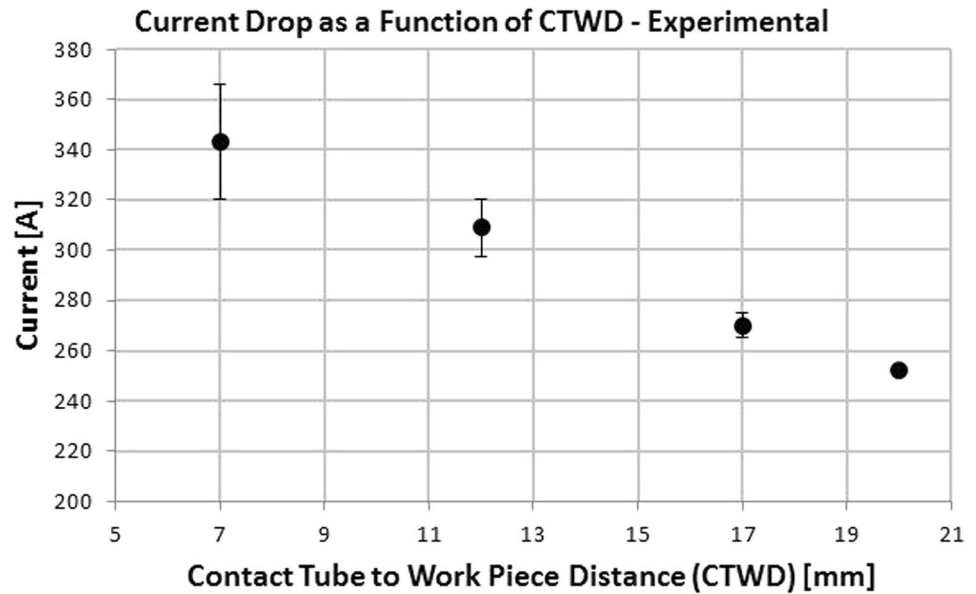


Table 2 Current and weld bead dimension values obtained in experimental procedure for correspondent CTWD

CTWD [mm]	Current (A)	Penetration (mm)	Width [mm]	Total fusion zone area [mm ²]	Dilution [%]
7	343	2.74	8.41	21.18	56
12	309	2.61	8.91	19.85	53
17	270	2.37	8.12	17.86	43
20	252	1.92	8.38	17.71	41

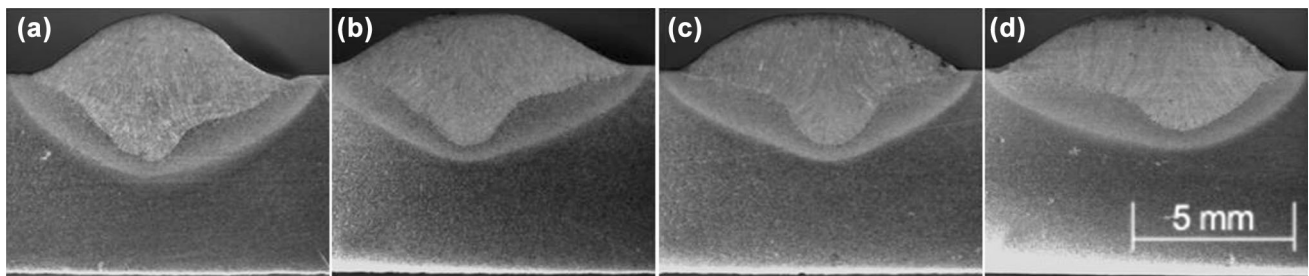


Fig. 7 Weld bead cross section. **a** CTWD = 7 mm, **b** CTWD = 12 mm, **c** CTWD = 17 mm, **d** CTWD = 20 mm

disturbances have great attractiveness. Thus, the present work consists in the first stage of the development of an adaptive system, able to mitigate weld discontinuities owing to stick out variation effects during MIG/MAG welding when CTWD oscillates. This stage is based on a preliminary approach of most relevant thermal and electrical variables behavior. This information is fundamental for control algorithms selection and development, which will aim at the ability to preserve arc stability and weld uniformity.

Current oscillations are a crucial factor for welding quality. From Lesnewich equation, current decay had a

nonlinear profile for stick out range from 1 to 40 mm. However, for both theoretical procedures performed, with stick out range from 5 to 20 mm, and experimental domain, for CTWD range from 7 to 20 mm, a straight line can be used as an approximation. Values of current drop in both approaches were similar, with average values of 6.5 A/mm in the theoretical curve, and 7.0 ± 1.4 A/mm, for the experimental one. Therefore, Lesnewich equation can be used as a starting point for control routines development in welding power sources, which reduces the need of experimental trials during adaptive systems development. This result was statistically proved through a hypothesis test.

A higher preheating degree was found for greater stick out values, despite lower current values. This could be certified through temperature profile from energy balance differential equation and can be explained due to higher Joule heating contribution. Voltage drop and electrode electrical resistance were also quantified, and presented a linear dependence with stick out. Linear relations are computationally efficient for control algorithms.

Macrographies pointed an expressive reduction in weld bead penetration for higher stick out lengths. This fact is associated with current reduction, and consequent electromagnetic forces, arc pressure and droplet impact intensity over weld pool (momentum).

Understanding of presented effects has an important role in the development of adaptive systems to increase arc regularity. Also not to be disregarded is the side conclusion that the present results may be useful to reinforce the alert to welding inspectors and operators that fewer modifications in torch conduction can lead to instabilities and weld defects.

References

1. Silva RHG (2005) Soldagem MIG/MAG em transferência metálica por curto-circuito controlado aplicada ao passe de raiz. Programa de Pós-Graduação em Engenharia Mecânica, Universidade Federal de Santa Catarina, Florianópolis
2. Roßmann F (2015) Advanced pulse welding characteristics. *Weld Cut* 14:12–14
3. Cruz JG, Torres EM, Alfaro SC (2015) A methodology for modeling and control of weld bead width in the GMAW process. *J Braz Soc Mech Sci Eng* 37:1529–1541
4. Nele L, Sarno E, Keshari A (2013) Modeling of multiple characteristics of an arc weld joint. *Int J Adv Manuf Technol* 69:1331–1341
5. Saraev Y (2014) The development and application of adaptive pulse-arc welding methods for construction and repair of pipelines (MEACS) Tomsk 16–18 October
6. Mvola B, Kah P, Martikainen J, Hiltunen E (2013) Applications and benefits of adaptive pulsed GMAW. *Mechanika* 19:694–701
7. Yan Z, Zhang G, Wun L (2011) Simulation and controlling for weld shape process in P-GMAW based on fuzzy logic. In: Proceedings of the 2011 IEEE international conference on mechatronics and automation august 7–10, Beijing
8. Silva RHG, Dutra JC, JrR Gohr (2008) Fundamentos científicos e tecnológicos para o desenvolvimento do processo MIG/MAG por curto-circuito controlado (CCC)—uma revisão da literatura. Parte 3 de 3: princípios dos sistemas MIG/MAG em curto-circuito com controle de corrente. *Soldagem e Inspeção* 13:70–81
9. Mendonça FK (2013) Evolução da técnica de seguimento de junta via sensoriamento do arco para operações de soldagem em posições forçadas. Programa de Pós-Graduação em Engenharia Mecânica, Universidade Federal de Santa Catarina, Florianópolis
10. Lesnewich A (1958) Control of melting rate and metal transfer in gas-shielded metal-arc welding part I—control of electrode melting rate. *Welding Research Supplement* 343–353
11. French IE (1984) Effects of electrode extension on deposit characteristics and metal transfer of E70T-4 electrodes. *Weld J* 63(3):167–172
12. Waszink JH, Van Den Heuvel GJPM (1982) Generation and heat flow in the filler metal in GMA welding. *Weld J* 61:269–280
13. Waszink JH, Van Den Heuvel GJPM (1979) Measurements and calculations of the resistance of the wire extension in arc welding. arc physics and weld pool behaviour international conference. May 8–10, London
14. Scotti A, Ponomarev V (2014) Soldagem MIG/MAG: melhor entendimento, melhor desempenho. Artiliber Editora Ltda, São Paulo
15. Essers WG, Walter R (1979) Some aspects of the penetration mechanisms in metal inert gas (MIG) welding. arc physics and weld pool behaviour international conference 8–10 London
16. Kim JW, Na SJ (1995) A study on the effect of contact tube-to-workpiece distance on weld pool shape in gas metal arc welding. *Weld J* 74(5):141–152
17. Traidia A, Roger F, Guyot E (2010) Optimal parameters for pulsed gas tungsten arc welding in partially and fully penetrated weld pools. *Int J Therm Sci* 49:1197–1208
18. Santana IJ, Modenesi PJ (2011) Modelagem matemática do processo de soldagem gmaw—transferência por voo livre. *Soldagem e Inspeção* 16:213–222
19. ASM (1990) ASM Metals Handbook, Physical properties of carbon and low alloy steels. ASM, Russell Township
20. Labsolda (2010) Vídeo Stick Out. <https://www.youtube.com/watch?v=uFWONovK1-Q>. Accessed 19 January 2017